LIMNOLOGY
and
OCEANOGRAPHY

ASLO

Limnol. Oceanogr. 61, 2016, 2045–2057

doi: 10.1002/lno.10352

H^+-driven increase in CO_2 uptake and decrease in HCO_3^- uptake explain coccolithophores' acclimation responses to ocean acidification

Dorothee M. Kottmeier,* Sebastian D. Rokitta, Björn Rost
Department of Marine Biogeosciences, Alfred Wegener Institute, Helmholtz Centre for Polar and Marine Research, Bremerhaven, Germany

Abstract

Recent ocean acidification (OA) studies revealed that seawater $[H^+]$ rather than $[CO_2]$ or $[HCO_3^-]$ regulate *short-term* responses in carbon fluxes of *Emiliania huxleyi*. Here, we investigated whether *acclimation* to altered carbonate chemistry modulates this regulation pattern and how the carbon supply for calcification is affected by carbonate chemistry. We acclimated *E. huxleyi* to *present-day* (ambient $[CO_2]$, $[HCO_3^-]$, and pH) and *OA* conditions (high $[CO_2]$, ambient $[HCO_3^-]$, low pH). To differentiate between the CO_2 and pH/H^+ effects, we also acclimated cells to *carbonation* (high $[CO_2]$ and $[HCO_3^-]$, ambient pH) and *acidification* (ambient $[CO_2]$, low $[HCO_3^-]$, and pH). Under these conditions, growth, production of particulate inorganic and organic carbon, as well as carbon and oxygen fluxes were measured. Under *carbonation*, photosynthesis and calcification were stimulated due to additional HCO_3^- uptake, whereas growth was unaffected. Such stimulatory effects are not apparent after short-term *carbonation*, indicating that cells adjusted their carbon acquisition during acclimation. Being driven by $[HCO_3^-]$, these regulations can, however, not explain typical OA effects. Under *acidification* and *OA*, photosynthesis stayed constant, whereas calcification and growth decreased. Similar to the short-term responses toward high $[H^+]$, CO_2 uptake significantly increased, but HCO_3^- uptake decreased. This antagonistic regulation in CO_2 and HCO_3^- uptake can explain why photosynthesis, being able to use CO_2 and HCO_3^-, often benefits from OA, whereas calcification, being mostly dependent on HCO_3^-, often decreases. We identified H^+ as prime driver of coccolithophores' acclimation responses toward OA. Acidified conditions seem to put metabolic burdens on the cells that result in decreased growth.

Emiliania huxleyi is the Earth's most dominant pelagic calcifier and known to be well adapted to shallow mixed-layer depths with high irradiances (Nanninga and Tyrrell 1996; Raitsos et al. 2006). Under these conditions, the species is able to form large monospecific blooms with cell concentrations of up to 10×10^7 cells L^{-1} (Holligan et al. 1993; Tyrrell and Merico 2004). In the process of calcification, CO_3^{2-} precipitates intracellularly with Ca^{2+} to form $CaCO_3$, leading to reduced seawater CO_3^{2-} levels and alkalinity. This production of particulate inorganic carbon (PIC) furthermore increases the partial pressure of carbon dioxide (pCO_2) of seawater and thereby counteracts the effect of photosynthetic production of particulate organic carbon (POC). The relative strength of calcification vs. photosynthesis therefore influences the biogeochemical CO_2 fluxes on regional and global scales (Broecker and Peng 1987; Rost and Riebesell 2004).

In the last decades, *E. huxleyi* has become an important model organism, especially because of its high sensitivity toward ocean acidification (OA; Raven and Crawfurd 2012; Read et al. 2013; Meyer and Riebesell 2015). This term describes the strong increase in CO_2 and the slight increase in HCO_3 levels (their sum is referred to as carbonation) as well as the decrease in CO_3^{2-} levels and pH (the latter corresponds to an increase in $[H^+]$ and is referred to as acidification), which result from the oceanic uptake of anthropogenic CO_2 (Wolf-Gladrow et al. 1999; Caldeira and Wickett 2003). A large number of laboratory and field studies on *E. huxleyi* and other coccolithophores found that OA leads to unaffected or stimulated photosynthesis, with impaired or unaffected calcification and growth, typically leading to decreased PIC: POC ratios (Raven and Crawfurd 2012; Kroeker et al. 2013; Meyer and Riebesell 2015). These responses can yet vary in magnitude, depending on genetic predisposition and other environmental boundary conditions such as light, temperature, or nutrient status (Zondervan

*Correspondence: Dorothee.Kottmeier@awi.de

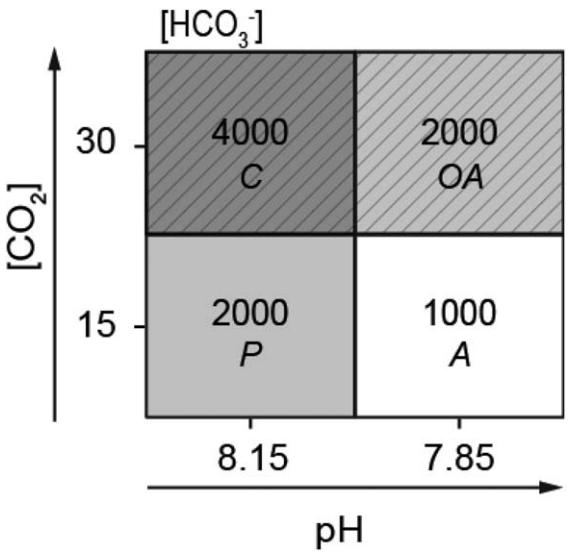

Fig. 1. Decoupled carbonate chemistry during acclimation of *Emiliania huxleyi* and during cellular flux measurements. Applied conditions were *present-day* (*P*; light grey), *carbonation* (*C*; dark grey, dashed), *acidification* (*A*; white) and *ocean acidification* (*OA*; light grey, dashed). Numbers inside the fields denote concentrations of HCO_3^-. Concentrations of CO_2 and HCO_3^- are given in μmol kg^{-1}.

2007; Langer et al. 2009; Lefebvre et al. 2012; Rokitta and Rost 2012; Sett et al. 2014; Xu and Gao 2015).

In first attempts to identify the chemical drivers of typical OA responses, *E. huxleyi* was acclimated to decoupled carbonate chemistry, under which carbonation and acidification effects could be distinguished (Bach et al. 2011, 2013). These acclimation studies revealed that POC and PIC production are both stimulated by carbonation, but are reduced when cells are acclimated to acidification. The antagonistic regulation of PIC production by carbonation and acidification was also indicated by a study of Fukuda et al. (2014), who showed that calcification is reduced under high $[H^+]$, but that this reduction can be overcome by additional HCO_3^- availability. A recent study investigated the mechanisms underlying short-term carbonation and acidification responses of present-day acclimated *E. huxleyi* by means of membrane-inlet mass spectrometry (Kottmeier et al. 2016). In this study, photosynthetic fluxes of *E. huxleyi* were shown to be relatively insensitive toward abrupt increases in CO_2 and HCO_3^- levels, i.e., when being exposed to carbonation for time scales of seconds to minutes. The fluxes were, however, very sensitive toward abrupt increases in H^+ levels, i.e., to acidification. Under the latter conditions, photosynthetic HCO_3^- uptake was strongly inhibited. Low-light acclimated cells were able to overcompensate this inhibition in HCO_3^- uptake with additional CO_2 uptake. High-light acclimated cells were unable to increase CO_2 uptake and photosynthesis therefore experienced a shortage in the supply inorganic carbon (C_i). These regulations could be different after an acclimation phase, during which cells adjust their metabolism to the altered conditions, e.g., by changing gene expression. Also, we are currently lacking information about C_i fluxes into calcification and their dependence on carbonation and acidification.

In order to understand the differences between *short-term* and *acclimation* responses toward carbonation and acidification, we here acclimated *E. huxleyi* to *present-day* (ambient $[CO_2]$, $[HCO_3^-]$, and pH) and *OA* conditions (high $[CO_2]$, ambient $[HCO_3^-]$, low pH). To differentiate between the CO_2 and pH/H^+ effects, we also acclimated cells to *carbonation* (high $[CO_2]$ and $[HCO_3^-]$, ambient pH) and *acidification* (ambient $[CO_2]$, low $[HCO_3^-]$, and pH; Fig. 1; Table 1). We assessed integrated responses in growth, elemental composition and POC and PIC production rates, and measured in vivo fluxes of O_2, CO_2, and HCO_3^- associated with photosynthesis and calcification under acclimation conditions. By comparing these responses with short-term responses (Kottmeier et al. 2016), we aimed to identify processes that were manifested or adjusted over the course of the acclimation.

Methods

Acclimations

Emiliania huxleyi strain RCC1216 was acclimated to four different carbonate chemistry conditions ("*present-day*", "*carbonation*", "*acidification*" and "*OA*"; Fig. 1; Table 1) under saturating irradiance (400 ± 30 μmol photons m^{-2} s^{-1}) for 7–14 d, i.e., 10–20 generations. Cells were grown as semicontinuous, dilute batch cultures in a 16 : 8 h light: dark cycle at 15 ± 1°C in sterile-filtered North Sea seawater (0.2 μm, Sartobran 300, Sartorius, Göttingen, Germany) with initial cell concentrations of 1000–3000 cells mL^{-1} and final concentrations of 40,000–60,000 cells mL^{-1}. Phosphate and nitrate were added to yield concentrations of ~7 and ~100 μmol kg^{-1}, respectively. Vitamins and trace metals were adjusted according to F/2 (Guillard and Ryther 1962). Cells were cultured on roller tables in sterilized, gas-tight 2 L borosilicate bottles (Duran Group, Mainz, Germany). Cultures were irradiated by daylight lamps (FQ 54W/965HO, Osram, Munich, Germany).

Irradiance was adjusted inside seawater-filled culturing bottles and measured with a Universal Light Meter (ULM 500, Walz, Effeltrich, Germany) using a 4π-sensor (US-SQS/L). Carbonate chemistry was adjusted by aerating the media with humidified, 0.2 μm-filtered air (Midisart 2000, Sartorius) containing a pCO_2 of 380 μatm in the *present-day* and *acidification* treatments, and a pCO_2 of 1000 μatm in the *carbonation* and *OA* treatments (Table 1). In the *acidification* and *carbonation* treatments, total alkalinity (TA) was adjusted by acid- or base addition (Table 1). Gas mixtures were produced with a gas flow controller (CGM 2000, MCZ Umwelttechnik, Bad Nauheim, Germany), mixing defined portions of pure CO_2 (Air Liquide, Duesseldorf, Germany) and CO_2-free air (Air purification system, Parker Zander, Kaarst, Germany). Carbonate chemistry of the media was controlled at the beginning as well as at the end

Table 1. Carbonate chemistry in the *present-day* (*P*), *carbonation* (*C*), *acidification* (*A*) and the *ocean acidification* (*OA*) treatments in cell-free media (Control), at the time of harvesting (Acc), and during cellular flux measurements with membrane-inlet mass spectrometry (MIMS). For acclimation conditions, attained pCO_2 (μatm), $[H^+]$ (nmol kg^{-1}), DIC (μmol kg^{-1}), $[CO_2]$ (μmol kg^{-1}), $[HCO_3^-]$ (μmol kg^{-1}), $[CO_3^{2-}]$ (μmol kg^{-1}), and $\Omega_{calcite}$ were calculated based on measured pH_{NBS} and TA (μmol kg^{-1}) using CO2sys (Pierrot et al. 2006). Results are reported for 15°C ($n \geq 3$; ± SD). Input parameters for CO2sys calculations were salinity (31), pressure (0.1 dbar), as well as phosphate (7 μmol kg^{-1}) and silicate (7 μmol kg^{-1}). Equilibrium constants by Mehrbach et al. (1973), refit by Dickson and Millero (1987) and dissociation constants for sulfuric acid by Dickson (1990) were applied. For MIMS conditions, carbonate chemistry was measured mass-spectrometrically (Badger et al. 1994; Schulz et al. 2007). The pCO_2 was calculated based on pH and $[CO_2]$ after Zeebe and Wolf-Gladrow (2001).

Treatment		pCO_2	pH_{NBS}	$[H^+]$	TA	DIC	$[CO_2]$	$[HCO_3^-]$	$[CO_3^{2-}]$	$\Omega_{calcite}$
P	Control	403 ± 4	8.13 ± 0.00	9.9 ± 0.1	2341 ± 4	2129 ± 4	15 ± 0	1961 ± 5	153 ± 1	3.7 ± 0.0
	Acc	384 ± 17	8.14 ± 0.01	9.9 ± 0.1	2280 ± 19	2068 ± 23	15 ± 1	1903 ± 25	151 ± 3	3.7 ± 0.1
	MIMS	486 ± 17	8.15 ± 0.01	9.3 ± 0.2	-	2323 ± 180	21 ± 3	2252 ± 264	160 ± 5	-
C	Control	868 ± 109	8.16 ± 0.02	9.5 ± 0.1	5317 ± 560	4899 ± 529	33 ± 4	4493 ± 489	373 ± 38	9.1 ± 0.9
	Acc	805 ± 84	8.18 ± 0.00	8.9 ± 0.3	5223 ± 527	4791 ± 491	31 ± 3	4379 ± 450	382 ± 39	9.3 ± 0.9
	MIMS	883 ± 13	8.18 ± 0.02	8.5 ± 0.4	-	4648 ± 69	36 ± 0	4263 ± 64	333 ± 5	-
A	Control	418 ± 12	7.83 ± 0.00	20.1 ± 0.2	1122 ± 19	1056 ± 19	16 ± 0	1002 ± 19	38 ± 0	0.9 ± 15
	Acc	410 ± 51	7.83 ± 0.04	19.0 ± 1.1	1119 ± 31	1052 ± 37	16 ± 2	997 ± 37	39 ± 2	1.0 ± 0.1
	MIMS	405 ± 12	7.88 ± 0.02	17.3 ± 0.8	-	1037 ± 31	17 ± 1	980 ± 30	38 ± 1	-
OA	Control	998 ± 15	7.78 ± 0.01	22.5 ± 0.2	2312 ± 2	2238 ± 2	38 ± 1	2127 ± 2	73 ± 1	1.8 ± 0.0
	Acc	964 ± 8	7.79 ± 0.00	22.1 ± 0.2	2287 ± 4	2211 ± 4	37 ± 0	2100 ± 4	73 ± 1	1.8 ± 0.0
	MIMS	942 ± 28	7.87 ± 0.02	17.8 ± 0.7	-	2357 ± 70	38 ± 1	2230 ± 67	85 ± 3	-

of the acclimation period, and was calculated based on pH_{NBS} and TA measurements using CO2sys (Table 1; Pierrot et al. 2006). Shifts in carbonate chemistry over the course of the experiment were small, i.e., drifts in pH were ≤ 0.02 units and TA as well as DIC drifted by $\leq 3\%$.

Measurements of pH were performed with a Metrohm pH meter (826 pH mobile, Metrohm, Filderstadt, Germany) using an Aquatrode Plus electrode with integrated temperature sensor (measurement reproducibility ± 0.01 pH units). TA was determined with potentiometric titration (TitroLine alpha plus, measurement reproducibility ± 7 μmol kg^{-1}, Schott Instruments, Mainz, Germany) of sterile-filtered samples (0.2 μm, cellulose acetate syringe filters, Thermo Fisher Scientific, Waltham, Massachusetts, U.S.A.) and was corrected with certified reference materials (CRM; provided by A. Dickson; Scripps Institution of Oceanography, U.S.A.). Dissolved inorganic carbon (DIC) was controlled with colorimetric measurements of sterile-filtered samples with a QuAAtro autoanalyser (measurement reproducibility ± 5 μmol kg^{-1}, Seal Analytical, Norderstedt, Germany) following the method of (Stoll et al. 2001).

Growth and production rates

Cellular quotas of POC, PIC, and particulate organic nitrogen (PON; pg cell^{-1}) were measured with an Automated Nitrogen Carbon Analyser mass spectrometer (ANCA-SL 20-20, Sercon Ltd., Crewe, UK). Known volumes of cell suspension were vacuum-filtered (−200 mbar relative to atmosphere) onto precombusted (12 h, 500°C) GF/F filters (1.2 μm; Whatman, Maidstone, UK) 6–8 h after the beginning of the light phase. POC filters were wetted with HCl (200 μL, 0.2 M) to remove calcite and subsequently dried overnight at 65°C prior to measurements. Cellular quotas of PIC were assessed as the difference in carbon quotas between acidified and non-acidified filters. Quotas of chlorophyll *a* (Chl *a*; pg cell^{-1}) were assessed by filtering defined volumes of cell suspension onto cellulose nitrate filters (0.45 μm, Sartorius, Göttingen, Germany), which were subsequently frozen in liquid nitrogen and stored at −80°C until analysis. Chl *a* was extracted in 90% acetone (v/v, Sigma, Munich, Germany) and determined fluorometrically (TD-700 fluorometer, Turner Designs, Sunnyvale, California, U.S.A.) according to Knap et al. (1996). The fluorometer was calibrated with an *Anacystis nidulans* Chl *a* standard (Sigma). Cell growth was determined by daily cell counting 6–8 h after the beginning of the light phase with a Coulter Counter (Beckman-Coulter, Fullerton, California, U.S.A.), and the growth constant μ (d^{-1}) was determined as:

$$\mu = \frac{\ln c_2 - \ln c_1}{t_2 - t_1} \quad (1)$$

with c_2 and c_1 being the cell concentrations (cells mL^{-1}) at the two sampling time points t_1 and t_2 (d). Production rates of POC and PIC (pg cell^{-1} d^{-1}) were approximated as

$$\text{POC production} = \text{POC quota} \cdot \mu \quad (2)$$

$$\text{PIC production} = \text{PIC quota} \cdot \mu \quad (3)$$

Cellular oxygen and carbon fluxes

Photosynthetic *real time* fluxes of oxygen (O_2) and C_i were measured by means of membrane-inlet mass spectrometry

(MIMS; Isoprime, GV Instruments, Manchester, UK) at conditions resembling the in situ carbonate chemistry (Table 1) and irradiance. Fluxes were estimated following the disequilibrium method by Badger et al. (1994). In this technique, calculations of photosynthetic CO_2 and HCO_3^- fluxes across the plasmalemma are based on the chemical disequilibrium between the two C_i species during their light-dependent uptake. To account for calcification, we followed the modifications introduced by Schulz et al. (2007) and Kottmeier et al. (2016) and applied measured PIC: POC ratios of the cells that were acclimated to the respective carbonate chemistry conditions. Prior to measurements, acclimated *E. huxleyi* cells were concentrated by gentle vacuum filtration (−200 mbar relative to atmosphere) over a polycarbonate filter (Isopore TSTP, 3 μm, Merck, Darmstadt, Germany). Culture medium was exchanged with 50 mM N,N-bis(2-hydroxyethyl)glycine (BICINE)-buffered DIC-free seawater medium of the appropriate pH, and 8 mL of the concentrated and buffered cell suspension (5–10 $\times$ 10^6 cells mL^{-1}) were transferred into the MIMS cuvette. Carbonate chemistry was adjusted by adding the corresponding concentrations of $NaHCO_3$ (Table 1). During a first dark phase prior to the actual measurement intervals, membrane-impermeable dextran-bound sulphonamide (25 μM, DBS; Synthelec, Lund, Sweden) was added to inhibit any potential activity of external carbonic anhydrase (CA; please note that this strain expresses hardly any external CA; S. D. Rokitta, unpubl. data). Chl *a* samples of the concentrated cell suspensions were taken to quantify the assayed biomass.

Fluxes of O_2 and C_i were measured in consecutive, 6-min light and dark phases in a temperature-controlled cuvette. Steady-state photosynthetic net O_2 evolution (*Phot*; μmol kg^{-1} min^{-1}) was measured in the light, whereas respiratory O_2 uptake (*Resp*; μmol kg^{-1} min^{-1}) was measured in the subsequent dark phase. Photosynthetic and respiratory O_2 fluxes were converted to C_i fluxes by applying a photosynthetic quotient (*PQ*) of 1.1 and a respiratory quotient of 1.0, respectively (Burkhardt et al. 2001; Kottmeier et al. 2016). C_i fluxes into calcification (Cal_{MIMS}; μmol kg^{-1} min^{-1}) were derived by multiplying photosynthetic net C_i fixation with light-phase normalized PIC: POC ratios ($PIC: POC_{light}$) in order to account for continuous respiration of POC during the 8-h dark phase (Schulz et al. 2007):

$$PIC : POC_{light} = \frac{\text{PIC quota}}{\text{POC quota}} \times \frac{16\ Phot - 8\ Resp}{16\ Phot} \quad (4)$$

$$Cal_{MIMS} = \frac{Phot}{PQ} \times PIC : POC_{light} \quad (5)$$

Cellular CO_2 uptake (CO_2up_{tot}; μmol kg^{-1} min^{-1}) was deduced from steady-state CO_2 drawdown in the light, and corrected for the simultaneous inter-conversion between CO_2 and HCO_3^- according to Badger et al. (1994). Because calcification is predominantly supplied by external HCO_3^- (Sikes et al. 1980; Rost et al. 2002), we assumed that the CO_2 uptake for calcification (CO_2up_{CaCO3}; μmol kg^{-1} min^{-1}) was 20% of overall Cal_{MIMS} (Kottmeier et al. 2016). Accordingly, HCO_3^- uptake for calcification ($HCO_3^-up_{CaCO3}$; μmol kg^{-1} min^{-1}) was assumed to be 0.8 $\times$ Cal_{MIMS}. In order to test how strongly the assumption of 20% CO_2 usage for calcification affects the estimated photosynthetic CO_2 and HCO_3^- fluxes, we performed a sensitivity study, which revealed that errors in this assumption would cause small offsets, but do not change the overall observed regulation patterns (data not shown). Photosynthetic CO_2 uptake (CO_2up_{PS}; μmol kg^{-1} min^{-1}) was calculated by subtracting CO_2up_{CaCO3} from overall cellular CO_2 uptake. The fraction of overall photosynthetic C_i uptake that is covered by CO_2 (fCO_2) was obtained according to Kottmeier et al. (2016). Photosynthetic HCO_3^- uptake ($HCO_3^-up_{PS}$; μmol kg^{-1} min^{-1}) was calculated as the difference between overall photosynthetic C_i uptake and photosynthetic CO_2 uptake. Total HCO_3^- uptake ($HCO_3^-up_{tot}$; μmol kg^{-1} min^{-1}) was calculated as the sum of HCO_3^- uptake for calcification and HCO_3^- uptake for photosynthesis. All rates were normalized to Chl *a*. For further details on the calculations of the photosynthetic fluxes, we refer to Kottmeier et al. (2016).

Statistics

All experiments were carried out in biological triplicates. Differences between the *present-day*, *carbonation*, *acidification*, and *OA* treatments were tested pairwise for significance by applying two-sided *t*-tests. Effects were considered statistically significant when *p*-values were ≤ 0.05. In the Figures and Table 2, significant differences were indicated by different lower-case characters (e.g., a and b). Values denoted by two letters (e.g., ab) represent data that are not significantly different from a and b.

Results

Integrated responses

Cellular growth was unaltered after acclimation to *carbonation*, but decreased from ~1.1 at *present-day* to ~1.0 d^{-1} after acclimation to *acidification* or *OA* (Fig. 2A; Table 2). Cellular POC production was increased under *carbonation* (~15%), but constant under *acidification* and slightly decreased (~10%) under *OA* (Fig. 2B; Table 2). Also PIC production was strongly stimulated under *carbonation* (~45%), but decreased under *acidification* and *OA* (~15%; Fig. 2C; Table 2). The ratio of PIC: POC increased by ~20% under *carbonation*, but decreased slightly under *acidification* and *OA* (Fig. 2D; ~10%). Cellular Chl *a* quotas and Chl *a*: POC ratios, as well as the ratio of POC: PON were not affected by carbonate chemistry (Table 2). Scanning electron microscopy did not reveal malformations of coccoliths under any of the acclimation conditions (data not shown).

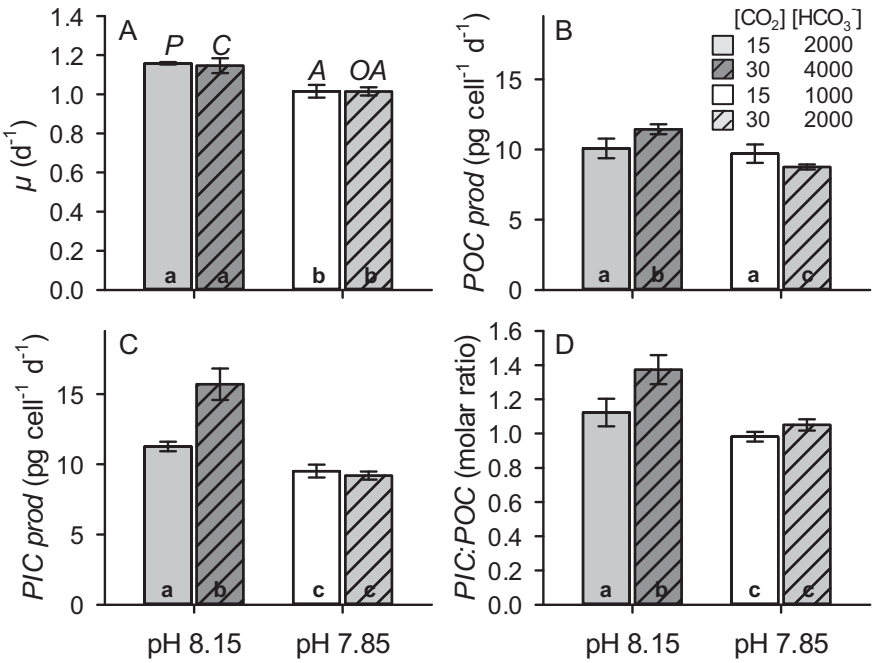

Fig. 2. Integrated responses to *present-day* (*P*; light grey), *carbonation* (*C*; dark grey, dashed), *acidification* (*A*; white) and *ocean acidification* (*OA*; light grey, dashed): (A) Cellular growth constants (μ), (B) production rates of particulate organic carbon (POC) (C) production rates of particulate inorganic carbon (PIC) and (D) PIC: POC ratios. Error bars indicate SD ($n = 3$). The different lower-case characters indicate significant differences between the data obtained at different carbonate chemistry conditions, e.g., data labeled "a" are statistically different from bars labeled "b" or "c."

Cellular fluxes

We measured cellular O_2 and C_i fluxes of the acclimated cells under in situ carbonate chemistry and light conditions in order to identify the alterations in fluxes that caused the alterations in the integrated responses. Similar to the POC production, also Chl *a*-normalized O_2 evolution (*Phot*) indicated that photosynthesis was increased under *carbonation* (~30%), but unaffected by *acidification* or *OA* (Fig. 3A; Table 2). Photosynthetic CO_2 uptake (CO_2up_{PS}) was low under *present-day*, became negative under *carbonation* (i.e., cells exhibited a CO_2 net efflux), but increased under *acidification* and *OA* (~600%; Fig. 3B; Table 2). Photosynthetic HCO_3^- uptake ($HCO_3^- up_{PS}$) was generally high and was further stimulated by *carbonation* (~45%), but decreased under *acidification* and *OA* (~50%; Fig. 3C; Table 2). As a consequence of these antagonistic regulations in CO_2 and HCO_3^- uptake, the ratio of photosynthetic CO_2 uptake to the overall photosynthetic C_i uptake (fCO_2) decreased from ~0.1 to ~−0.1 under *carbonation*, but increased to ~0.4 under *acidification* and *OA* (Fig. 3D; Table 2). Respiration (*Resp*) and the ratio of net photosynthesis to respiration (*Phot: Resp*) were relatively constant in all applied carbonate chemistry treatments (Table 2).

Calcification as estimated from light-normalized PIC: POC ratios and MIMS measurements (Cal_{MIMS}) strongly increased under *carbonation* (~60%), but apparently stayed constant under *acidification* and *OA* (Fig. 3E; Table 2). Yet, CalMIMS seemed to be slightly decreased in both low-pH treatments (Fig. 3E; Table 2). Also CO_2 and HCO_3^- uptake for calcification (CO_2up_{CaCO3}, $HCO_3^- up_{CaCO3}$) increased under *carbonation* (~60%), but remained relatively constant under *acidification* and *OA* (Fig. 3F; Table 2). Total cellular CO_2 uptake (CO_2up_{tot}), i.e., the sum of CO_2 uptake for photosynthesis and for calcification, was unaffected by *carbonation*, whereas it strongly increased under *acidification* and *OA* (~150%; Table 2). Total cellular HCO_3^- uptake ($HCO_3^- up_{tot}$) was increased under *carbonation* (~50%), whereas it decreased under *acidification* and *OA* (~25%; Fig. 3G; Table 2). The ratio of HCO_3^- uptake for calcification to HCO_3^- uptake for photosynthesis ($HCO_{3\ CaCO3}^-$: $HCO_{3\ PS}^-$) was not affected by *carbonation*, but strongly increased under *acidification* and *OA* (~50%, Fig. 3H; Table 2).

Discussion

In this study, we measured the differential effects of acclimation to carbonation and acidification on growth, elemental composition and production rates in high-light grown *E. huxleyi*. In order to explain the observed integrated cellular responses, we measured the in vivo O_2, CO_2, and HCO_3^- fluxes of the acclimated cells under in situ conditions by means of MIMS.

Acclimation to *carbonation* boosts POC and PIC production by stimulating the uptake of HCO_3^-

Rates of POC production were strongly increased in the *carbonation* treatment, but were relatively unaffected under

Table 2. Integrated responses and underlying cellular fluxes of *Emiliania huxleyi* in the *present-day* (*P*), *carbonation* (*C*), *acidification* (*A*), and *ocean acidification* (*OA*) treatments: Different lower-case characters in superscript indicate statistically significant differences between the fluxes obtained at the different the carbonate chemistry conditions.

Parameter (unit)	*P*	*C*	*A*	*OA*
μ (d^{-1})	1.16 ± 0.01^{a}	1.15 ± 0.04^{a}	1.02 ± 0.03^{b}	1.01 ± 0.02^{b}
POC quota (pg $cell^{-1}$)	8.9 ± 0.6^{a}	10.2 ± 0.3^{b}	9.7 ± 0.7^{ab}	8.9 ± 0.2^{a}
POC production (pg $cell^{-1}$ d^{-1})	10.1 ± 0.7^{a}	11.4 ± 0.4^{b}	9.7 ± 0.7^{a}	8.8 ± 0.2^{c}
PIC quota (pg $cell^{-1}$)	10.0 ± 0.3^{a}	14.0 ± 1.0^{b}	9.5 ± 0.5^{a}	9.5 ± 0.3^{c}
PIC production (pg $cell^{-1}$ d^{-1})	11.3 ± 0.3^{a}	15.7 ± 1.1^{b}	9.5 ± 0.5^{c}	9.2 ± 0.3^{c}
PIC: POC (molar ratio)	1.12 ± 0.08^{a}	1.37 ± 0.08^{b}	0.98 ± 0.03^{c}	1.05 ± 0.03^{a}
PIC: POC_{light} (molar ratio)	0.87 ± 0.02^{a}	1.15 ± 0.03^{b}	0.82 ± 0.06^{a}	0.88 ± 0.02^{a}
Chl *a* quota (pg $cell^{-1}$)	0.13 ± 0.01^{a}	0.13 ± 0.01^{a}	0.12 ± 0.01^{a}	0.12 ± 0.01^{a}
Chl *a*: POC (pg pg^{-1})	0.014 ± 0.001^{a}	0.013 ± 0.001^{a}	0.013 ± 0.004^{a}	0.014 ± 0.002^{a}
PON quota (pg $cell^{-1}$ d^{-1})	1.5 ± 0.1^{a}	1.7 ± 0.2^{a}	1.8 ± 0.1^{a}	1.6 ± 0.1^{a}
POC: PON (molar ratio)	6.9 ± 0.2^{a}	6.8 ± 0.4^{a}	6.9 ± 0.3^{a}	6.6 ± 0.2^{a}
Phot (μmol (mg Chl *a*)$^{-1}$ h^{-1})	284 ± 41^{a}	371 ± 11^{b}	268 ± 41^{a}	295 ± 38^{a}
μ_{MIMS} (d^{-1})	1.06 ± 0.15^{a}	1.22 ± 0.04^{a}	0.88 ± 0.13^{a}	1.07 ± 0.12^{a}
CO_2up_{PS} (μmol (mg Chl *a*)$^{-1}$ h^{-1})	15 ± 11^{a}	-30 ± 17^{b}	93 ± 21^{c}	105 ± 20^{c}
$HCO_3^- up_{PS}$ (μmol (mg Chl *a*)$^{-1}$ h^{-1})	244 ± 34^{a}	368 ± 27^{b}	151 ± 23^{c}	163 ± 53^{c}
fCO_2	0.06 ± 0.03^{a}	-0.09 ± 0.05^{b}	0.38 ± 0.05^{c}	0.40 ± 0.13^{c}
Cal_{MIMS}	237 ± 34^{a}	390 ± 18^{b}	202 ± 42^{a}	222 ± 32^{a}
CO_2up_{CaCO3} (μmol (mg Chl *a*)$^{-1}$ h^{-1})	47 ± 7^{a}	78 ± 4^{b}	40 ± 8^{a}	50 ± 2^{a}
$HCO_3^- up_{CaCO3}$ (μmol (mg Chl *a*)$^{-1}$ h^{-1})	189 ± 28^{a}	312 ± 15^{b}	161 ± 34^{a}	178 ± 25^{a}
CO_2up_{tot} (μmol (mg Chl *a*)$^{-1}$ h^{-1})	57 ± 15^{a}	48 ± 14^{b}	134 ± 29^{a}	156 ± 20^{b}
$HCO_3^- up_{tot}$ (μmol (mg Chl *a*)$^{-1}$ h^{-1})	448 ± 32^{a}	679 ± 41^{b}	312 ± 54^{c}	352 ± 80^{c}
$HCO_3^- up_{CaCO3}$: $HCO_3^- upt_{PS}$	0.77 ± 0.03^{a}	0.85 ± 0.03^{a}	1.07 ± 0.15^{b}	1.22 ± 0.28^{b}
Resp (μmol (mg Chl *a*)$^{-1}$ h^{-1})	100 ± 27^{a}	107 ± 12^{a}	77 ± 16^{a}	85 ± 4^{a}
Phot: Resp	3.0 ± 0.8^{a}	3.5 ± 0.4^{a}	3.6 ± 1.1^{a}	3.5 ± 0.4^{a}

acidified conditions, i.e., in the *acidification* and *OA* treatments (Fig. 2B). The increase in biomass buildup under *carbonation* was also reflected in elevated rates of photosynthetic net O_2 evolution (Fig. 3A). Besides POC production, also PIC production and the MIMS-based estimates of calcification were significantly elevated under *carbonation* (Figs. 2C, 3E, 4B). The carbonation-driven increase in PIC production was larger than the increase in POC production, i.e., PIC: POC ratios increased (Fig. 2D; Table 2). This suggests that, when photosynthesis is substrate-saturated, the residual C_i is directed towards calcification. A redirection of C_i from photosynthesis to calcification was also observed under nutrient limitation, when cells cannot sustain photosynthetic biomass production and excess C_i is therefore available (Paasche and Brubak 1994; Van Bleijswijk et al. 1994; Paasche 1998). On the other hand, PIC: POC ratios were shown to decrease when DIC levels become too low to sustain both processes (Buitenhuis et al. 1999; Zondervan et al. 2002; Bach et al. 2013). Under these conditions, maintaining photosynthesis seems to be more important than sustaining calcification. Apparently, increased calcification acts as a "sink" for excess C_i, while decreased calcification acts as a C_i "source" for photosynthesis when intracellular C_i becomes sparse.

By measuring cellular CO_2 and HCO_3^- fluxes, the effects of carbonation on photosynthesis and calcification (Figs. 2B,C, 3A,E) could be attributed to a stimulated HCO_3^- uptake supplying these processes (Figs. 3C,F, 4B). Cellular and photosynthetic CO_2 uptake were meanwhile unaffected by *carbonation*. Stimulating carbonation effects are in line with the studies of Bach et al. (2011, 2013) and Buitenhuis et al. (1999), who found that POC and PIC production are, at constant pH, correlated with external [HCO_3^-]. The flux regulations after *acclimation* to carbonation, however, differed from those of present-day acclimated cells exposed to carbonation over *short* time scales, where neither CO_2 uptake nor HCO_3^- uptake were stimulated (Kottmeier et al. 2016). These differences indicate that cells, when being exposed to carbonation over several generations, adjust their metabolism to allow for higher HCO_3^- uptake, especially when light-energization is sufficient (Price et al. 2008). Higher HCO_3^- uptake rates could be achieved by increasing the number of HCO_3^- transporters and/or by shifting from high-affine forms with low transport capacities to low-affinity forms with high transport capacities (Eberlein et al. 2014). Genes involved in C_i uptake were indeed shown to be differentially expressed under changing DIC levels (Bach et al. 2013). Such carbonation

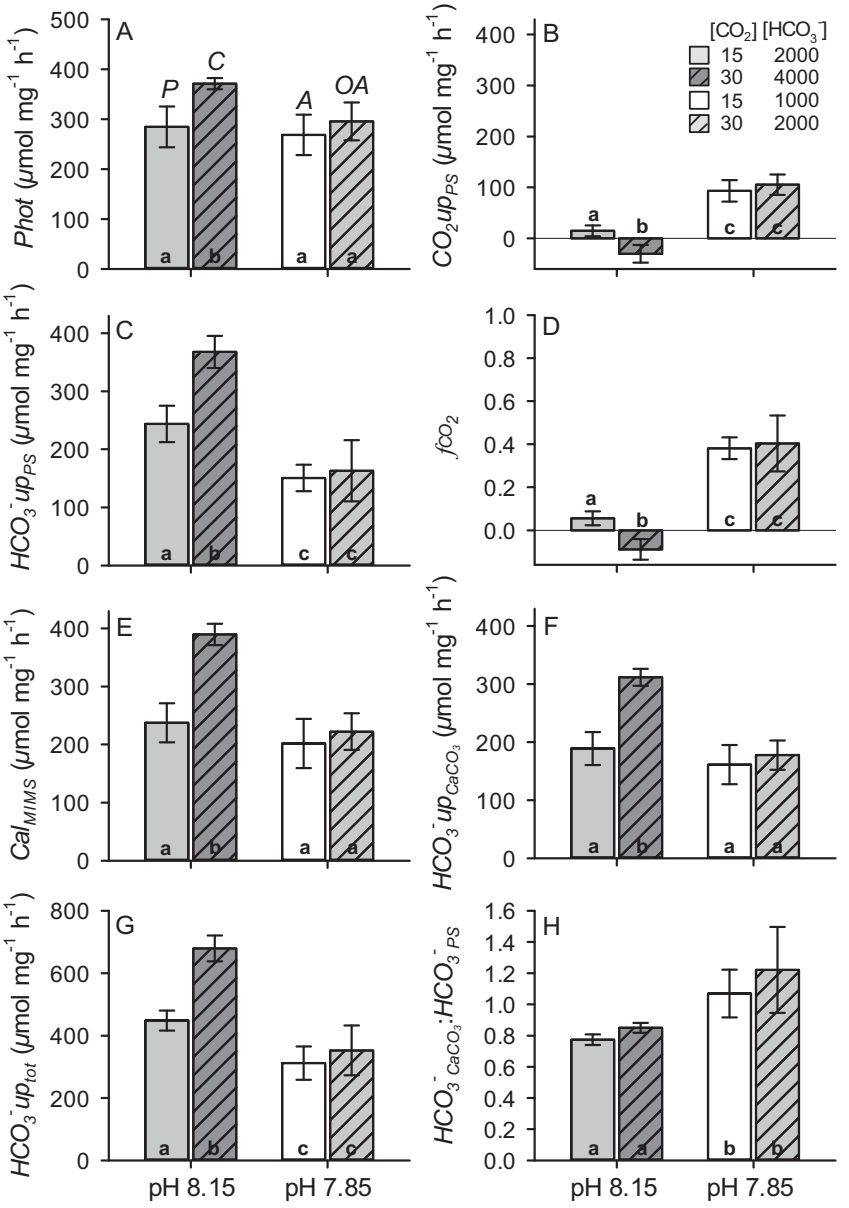

Fig. 3. Cellular O_2 and C_i fluxes of *Emiliania huxleyi* in the *present-day* (*P*; light grey), *carbonation* (*C*; dark grey, dashed), *acidification* (*A*; white), and *ocean acidification* (*OA*, light grey, dashed) treatments: (A) photosynthetic net O_2 evolution (*Phot*), (B) photosynthetic CO_2 uptake (CO_2up_{PS}), (C) photosynthetic HCO_3^- uptake ($HCO_3^-up_{PS}$), (D) ratio of photosynthetic CO_2 uptake to overall photosynthetic C_i uptake (fCO_2), (E) calcification rates (Cal_{MIMS}), (F) HCO_3^- uptake for calcification ($HCO_3^-up_{CaCO3}$), (G) Total HCO_3^- uptake ($HCO_3^-up_{tot}$), (H) Ratio of HCO_3^- uptake for calcification to HCO_3^- uptake for photosynthesis ($HCO_3^-{}_{CaCO3}$: $HCO_3^-{}_{PS}$). All rates were normalized to Chl *a*. Error bars indicate SD ($n = 3$). Different lower-case characters indicate significant differences between the fluxes obtained at different carbonate chemistry conditions.

effects may have been of importance in the Cretaceous when coccolithophores thrived, because at these times TA, DIC, and pH were considerably higher than today (Stanley et al. 2005; Hönisch et al. 2012). However, under the OA scenarios expected for the future, carbonation mainly involves increases in $[CO_2]$ with relatively small increases in $[HCO_3^-]$. Consequently, typical OA responses observed in coccolithophores (i.e., increased or unaffected POC production, decreased or unaffected PIC production and decreased PIC : POC ratios) cannot be explained by this HCO_3^--driven stimulation of POC and PIC production observed here, but must rather derive from acidification.

Acclimation to *acidified conditions* causes opposing regulations of photosynthetic HCO_3^- uptake and CO_2 uptake

Photosynthesis in *E. huxleyi* was relatively unaffected in both high $[H^+]$ treatments: Rates of POC production stayed

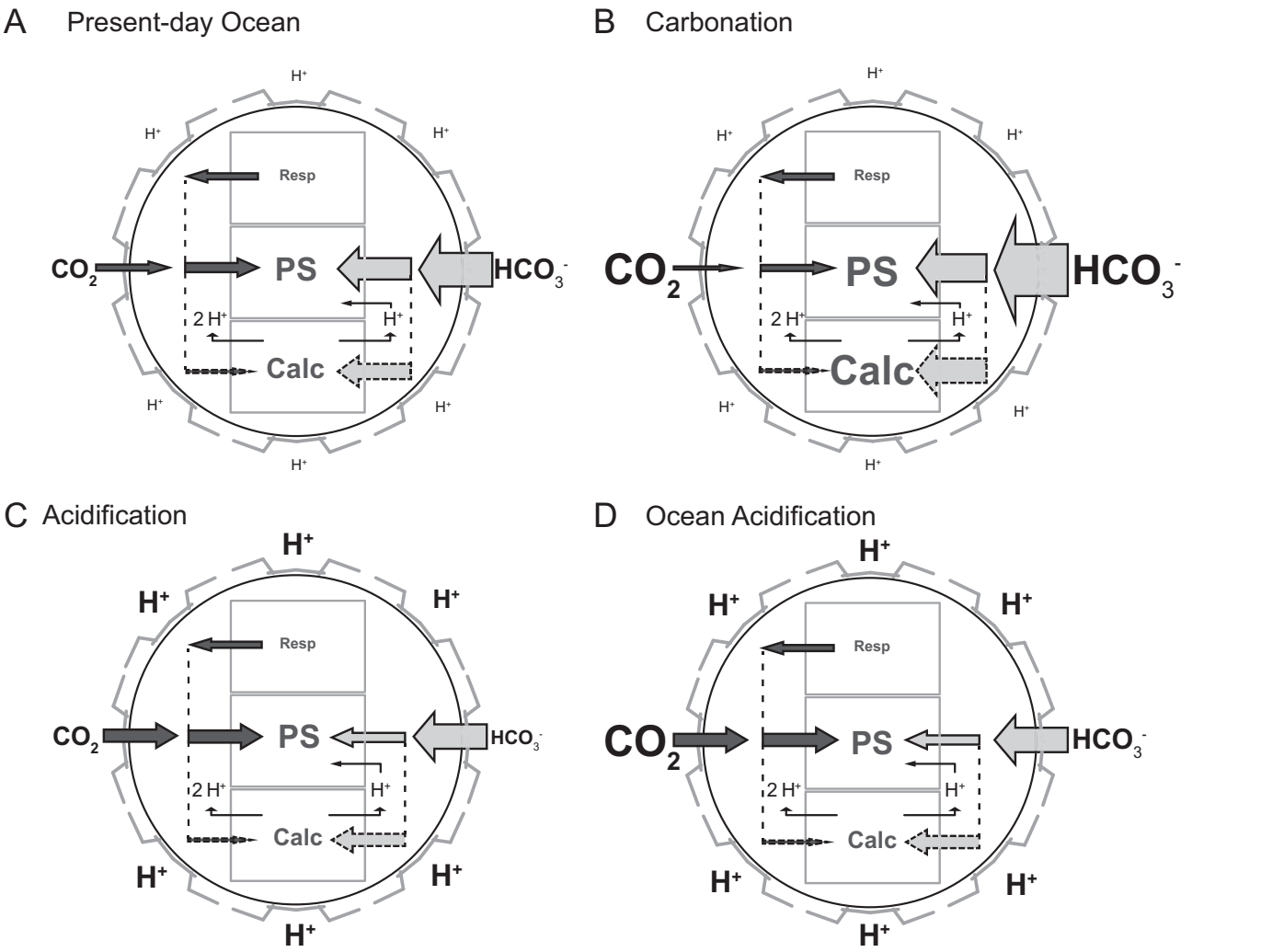

Fig. 4. Schematic illustration of C_i fluxes in *Emiliania huxleyi* acclimated to different carbonate chemistry settings under high irradiances: (A) Under *present-day* conditions, HCO_3^- is the main external substrate for photosynthesis and calcification. Fluxes of HCO_3^- into photosynthesis are slightly higher than HCO_3^- fluxes into calcification, leading to a small consumption of H^+ by photosynthesis. (B) Under *carbonation*, photosynthesis and calcification are both stimulated by increased HCO_3^- uptake. The increase in calcification is stronger than in photosynthesis, indicating that excess C_i is directed into calcification. The uptake of CO_2 is slightly downscaled, indicating that photosynthesis is largely independent of external [CO_2]. (C) Under *acidification*, cells maintain constant rates of photosynthesis, whereas calcification is slightly reduced. The photosynthetic C_i requirements are covered by increased proportions of CO_2 uptake, compensating for the reduced uptake of HCO_3^-. The decrease in calcification is likely caused by an inhibited cellular HCO_3^- transport. The ratio of HCO_3^- uptake for calcification vs. HCO_3^- uptake for photosynthesis increases, implying excess production of H^+. (D) Under *OA*, fluxes are basically equal to the fluxes in the *acidification* treatment, indicating that under typical OA scenarios where overall DIC levels are relatively unaffected, acidification effects are more pronounced than carbonation effects. Please note: Sizes of arrows are proportional with the measured fluxes under in situ conditions. Dashed arrows represent fluxes that were estimated based on measured PIC : POC ratios at the given conditions.

unaltered after acclimation to *acidification* and only slightly decreased after acclimation to *OA* (Fig. 2B). Also, rates of net O_2 evolution were unaltered in these low-pH treatments (Fig. 3A). The rather small acidification-sensitivity of high-light grown cells is in line with a previous acclimation study, which found OA responses to become less pronounced with increasing light intensities (Rokitta and Rost 2012). The acclimation responses observed here, however, were different from short-term responses: When high-light grown *E. huxleyi* was exposed to high [H^+] over time scales of minutes, net O_2 evolution significantly decreased (Kottmeier et al. 2016). This decrease was shown to be caused by an impairment of HCO_3^- uptake at concomitantly unaltered CO_2 uptake, leading to an overall decrease in cellular C_i uptake and thus insufficient CO_2 supply at RubisCO. In the current *acclimation* study, such detrimental H^+ effects on overall C_i uptake are not apparent. Instead, *E. huxleyi* was able to reestablish sufficiently high C_i uptake by mitigating the inhibitory H^+

effect on HCO_3^- uptake and slightly increasing CO_2 uptake for photosynthesis (Fig. 3B,C; cf. Fig. 3B,D in Kottmeier et al. 2016). However, the modified CO_2-concentrating mechanism (CCM), or other cellular adjustments under low pH, seem to impose a metabolic burden that result in lowered growth (Fig. 2A).

Despite the apparent insensitivity of photosynthesis to acidified conditions, the associated CO_2 and HCO_3^- supply was strongly affected when cells were acclimated to *acidification* and *OA*: Photosynthetic and also total cellular CO_2 uptake were significantly stimulated in both low-pH treatments, whereas photosynthetic and total cellular HCO_3^- uptake were significantly decreased (Figs. 3B,C,G, 4C,D). The shift in the photosynthetic C_i source is in line with the increased CO_2 usage observed under short-term exposure to high $[H^+]$ (Kottmeier et al. 2014, 2016) and shows that typical OA responses are driven by acidification rather than by carbonation, also after acclimation. The stimulatory OA effects on photosynthesis have often been attributed to the increased seawater CO_2 levels that were thought to enhance diffusive supply for RubisCO. Our results show that this stimulation in CO_2 uptake is actually driven by increased seawater H^+ levels. The H^+-dependent transition from HCO_3^- uptake to CO_2 uptake may decrease the cells' energetic costs, because HCO_3^- uptake is energy-driven in *E. huxleyi* (Kottmeier et al. 2016), while CO_2 is thought to enter phytoplankton cells primarily by diffusion (Giordano et al. 2005; Holtz et al. 2015a; Raven and Beardall 2016). Respiration, being an indicator for cellular energy demand, was indeed slightly, but insignificantly downscaled under acidified conditions (Table 2). However, overall growth was concomitantly also reduced and no obvious reinvestments into other processes, e.g., into POC or PIC production, were observed (Figs. 2A,B,C). Thus, there were no indications for a more efficient energy budgeting, at least at the high light levels applied here.

H^+-driven shift in C_i source can explain the often observed decrease in PIC : POC ratios under OA

Because calcification depends on the same HCO_3^- uptake mechanism as photosynthesis (Paasche 1964; Holtz et al. 2015b), it is plausible that calcification is also affected by the H^+-driven impairment of the cellular HCO_3^- uptake (Fig. 4C,D). Our data revealed that PIC production was indeed slightly decreased under *acidification* and *OA* (Fig. 2C). The relatively small decrease is likely a result of the applied high light intensities (Rokitta and Rost 2012). The reason why this decrease could not be fully resolved by the MIMS measurements (CalMIMS; Fig. 3F), is possibly that the uncertainties were larger than the effects. An interaction of a H^+-driven decrease in calcification (as seen under *acidification* and *OA*) and a HCO_3^--driven increase in calcification (as seen under *carbonation*) explains the often observed pseudo-correlation with the carbonate saturation state (Ω), which has been discussed recently (Bach 2015; Cyronak et al. 2015; Rickaby et al. 2016).

A decreased HCO_3^- supply for calcification, next to the increased CO_2 supply for photosynthesis and the prioritization of photosynthesis over calcification under C_i-shortage, may explain the decreases in PIC: POC ratios under OA that were often observed in *E. huxleyi* and other coccolithophores (Raven and Crawfurd 2012; Meyer and Riebesell 2015). Depending on species- and strain-specific features (e.g., size and morphotype) and environmental conditions (e.g., irradiance, nutrient status, and temperature), either the positive H^+ effect on CO_2 uptake for photosynthesis or the negative H^+ effect on cellular HCO_3^- uptake may overweigh. As a consequence, POC production can be stimulated (e.g., Riebesell et al. 2000; Zondervan et al. 2002), remain constant (e.g., Langer et al. 2009; Müller et al. 2015) or be decreased (e.g., Fiorini et al. 2011; Müller et al. 2015). Because PIC production is mainly affected by the impairment of the HCO_3^- uptake, it typically decreases (e.g., Riebesell et al. 2000; Zondervan et al. 2002; Langer et al. 2009; Müller et al. 2015) or stays constant under OA (e.g., Zondervan et al. 2002; Langer et al. 2009; Fiorini et al. 2011). At times, when photosynthesis benefits from a H^+-driven increase in CO_2 uptake, more HCO_3^- could be directed from POC to PIC production, which could even explain beneficial OA effects on calcification (e.g., Iglesias-Rodriguez et al. 2008).

The above described processes also explain the pCO_2 optimum curvature of PIC and POC production that are often observed in coccolithophores (e.g., Langer et al. 2006; Sett et al. 2014; Bach et al. 2015; Zhang et al. 2015). At very high pCO_2, the negative H^+ effect on HCO_3^- uptake overweighs the stimulatory H^+ effect on CO_2 uptake, and consequently, production rates decrease. The recently observed shift of production optima towards lower pCO_2 with increasing acclimation light (Zhang et al. 2015) could be a consequence of the fact that the H^+-driven stimulation in photosynthetic CO_2 uptake becomes less pronounced with increasing light (Kottmeier et al. 2016). This would also explain why high-light grown phytoplankton can already experience an energetic overload at pCO_2 levels, at which low-light acclimated cells still function properly (Gao et al. 2012; Hoppe et al. 2015; Zhang et al. 2015; Kottmeier et al. 2016).

Decreased growth under elevated $[H^+]$ and high irradiance poses a risk for *E. huxleyi* in the future ocean

In the applied low-pH treatments, *E. huxleyi* was, despite the strong flux regulations, able to maintain rather constant photosynthesis, calcification, respiration, POC : PON ratios and Chl *a* quotas (Table 2). This was likely possible due to the high energization (400 μmol m^{-2} s^{-1}). However, the ability to maintain these traits seemed to be accomplished at the expense of cellular growth (Fig. 2A; cf., Langer et al. 2009; Rokitta and Rost 2012; Kottmeier et al. 2014). Under acidified conditions, cells may, for example, face increased

costs for acid-base regulation, because the decreased seawater pH directly leads to a decreased cytosolic pH (Mackinder et al. 2010; Suffrian et al. 2011; Taylor et al. 2011; Rokitta et al. 2012). Our flux measurements revealed higher biological "H^+ generation" in the low-pH treatments, i.e., the ratio of HCO_3^- flux into calcification (a pathway that generates H^+) over the HCO_3^- flux into photosynthesis (a pathway that consumes H^+) was significantly increased (Figs. 3H, 4C,D; cf., Holtz et al. 2015b; Kottmeier et al. 2016). Such a H^+ imbalance may become even larger with increasing irradiances, because the overall HCO_3^- fluxes are higher under these conditions, and consequently more H^+ are released intracellularly. We also observed that *E. huxleyi's* ability to redistribute C_i between the process of photosynthesis and calcification becomes smaller under OA, because the overall HCO_3^- uptake capacity decreased. This comes into play especially under high light, when photosynthesis cannot use CO_2 as alternative C_i source (Kottmeier et al. 2016). Lastly, the inhibited growth may also derive from an energetic overload under these conditions, because the high $[H^+]$ impairs the "costly" part of the CCM, i.e., HCO_3^- uptake, and surplus energy under high irradiance cannot be dissipated by HCO_3^- pumping (Tchernov et al. 1997; Hoppe et al. 2015).

The future of coccolithophores is often predicted based on their sensitivity in POC and PIC production rates. Changes in growth, even when being seemingly small, can yet have large consequences that are not necessarily reflected in production rates: The observed drop in growth under high $[H^+]$ from $\sim$1.15 d^{-1} to 1.00 d^{-1} would, for example, lead to a 50% discrepancy in the POC buildup of a population over the course of only 4 d. Even though *E. huxleyi* is known to exhibit an exceptional tolerance for high irradiances (Nanninga and Tyrrell 1996; Nielsen 1997; Trimborn et al. 2007; Ragni et al. 2008), the decreased growth under high light and low pH, and the higher susceptibility to photoinhibition (Kottmeier et al. 2016), suggest that under future OA, *E. huxleyi* will be close to the upper limit of its physiological scope. Under the dynamic light in natural environments, the balancing of variable C_i demands with the limited C_i uptake capacities under OA may become even more challenging (Rost et al. 2006; Jin et al. 2013b; Hoppe et al. 2015; Xing et al. 2015; Xu and Gao 2015). Because *E. huxleyi* forms blooms in summer, i.e., in high-light conditions, the species may face difficulties in sustaining its growth and partially lose its exceptional blooming capacities in the future ocean.

Conclusion

In this study, we confirmed the strong acidification-dependent regulations of C_i fluxes in *E. huxleyi* that were earlier observed after direct exposure to high $[H^+]$ (Kottmeier et al. 2014, 2016). We found that, at typical OA scenarios, acidification effects dominate over carbonation effects. The verification of the strong H^+ dependency in flux regulations, also after acclimation for 10–20 generations, now allows explaining the integrated OA responses of coccolithophores measured in the last decades: The common pattern of decreased PIC: POC ratios under OA can be attributed to the H^+-driven decrease in cellular HCO_3^- uptake and the concomitant increase in CO_2 uptake. Because calcification largely relies on HCO_3^- as external C_i source, it is generally more affected by the decrease in HCO_3^- uptake and therefore decreases relative to photosynthesis. Overall, the strength of the antagonistic H^+ effects on HCO_3^- and CO_2 uptake can vary and thereby determine the magnitude and direction of OA responses. It remains to be tested whether the intrinsic H^+-dependency can be overcome by adaptation (Lohbeck et al. 2012; Jin et al. 2013a) and whether this could shift the "physiological limits" of coccolithophores.

References

Bach, L. T. 2015. Reconsidering the role of carbonate ion concentration in calcification by marine organisms. Biogeosci. Discuss. **12**: 6689–6722. doi:10.5194/bgd-12-6689-2015

Bach, L. T., U. Riebesell, and K. G. Schulz. 2011. Distinguishing between the effects of ocean acidification and ocean carbonation in the coccolithophore *Emiliania huxleyi*. Limnol. Oceanogr. **56**: 2040–2050. doi:10.4319/lo.2011.56.6.2040

Bach, L. T., L. C. Mackinder, K. G. Schulz, G. Wheeler, D. C. Schroeder, C. Brownlee, and U. Riebesell. 2013. Dissecting the impact of CO_2 and pH on the mechanisms of photosynthesis and calcification in the coccolithophore *Emiliania huxleyi*. New Phytol. **199**: 121–134. doi:10.1111/nph.12225

Bach, L. T., U. Riebesell, M. A. Gutowska, L. Federwisch, and K. G. Schulz. 2015. A unifying concept of coccolithophore sensitivity to changing carbonate chemistry embedded in an ecological framework. Prog. Oceanogr. **135**: 125–138. doi:10.1016/j.pocean.2015.04.012

Badger, M. R., K. Palmqvist, and J. W. Yu. 1994. Measurement of CO_2 and HCO_3^- fluxes in cyanobacteria and microalgae during steady-state photosynthesis. Physiol. Plant. **90**: 529–536. doi:10.1111/j.1399-3054.1994.tb08811.x

Broecker, W. S., and T. H. Peng. 1987. The role of $CaCO_3$ compensation in the glacial to interglacial atmospheric CO_2 change. Global Biogeochem. Cycles **1**: 15–29. doi:10.1029/GB001i001p00015

Buitenhuis, E. T., H. J. W. De Baar, and M. J. W. Veldhuis. 1999. Photosynthesis and calcification by *Emiliania huxleyi* (Prymnesiophyceae) as a function of inorganic carbon species. J. Phycol. **35**: 949–959. doi:10.1046/j.1529-8817.1999.3550949.x

Burkhardt, S., G. Amoroso, U. Riebesell, and D. Sultemeyer. 2001. CO_2 and HCO_3^- uptake in marine diatoms

acclimated to different CO_2 concentrations. Limnol. Oceanogr. **46**: 1378–1391. doi:10.4319/lo.2001.46.6.1378

Caldeira, K., and M. E. Wickett. 2003. Anthropogenic carbon and ocean pH—the coming centuries may see more oceanic acidification than the past 300 million years. Nature **425**: 365. doi:10.1038/425365a

Cyronak, T., K. G. Schulz, and P. L. Jokiel. 2015. The Omega myth: What really drives lower calcification rates in an acidifying ocean. ICES J. Mar. Sci. Journal du Conseil fsv075: 1–5. doi:10.1093/icesjms/fsv075

Dickson, A. G., and F. J. Millero. 1987. A comparison of the equilibrium constants for the dissociation of carbonic acid in seawater media. Deep-Sea Res Pt I **34**: 1733–1743. doi:10.1016/0198-0149(87)90021-5

Dickson, A. G. 1990. Standard potential of the reaction: $AgCl(s) + {}^1/_2 H_2(g) = Ag(s) + HCl(aq)$, and the standard acidity constant of the ion HCO_4^- in synthetic seawater from 273.15 to 318.15 K. J. Chem. Thermodynamics **22**: 113–127. doi:10.1016/0021-9614(90)90074-Z

Eberlein, T., D. B. Van De Waal, and B. Rost. 2014. Differential effects of ocean acidification on carbon acquisition in two bloom-forming dinoflagellate species. Physiol. Plant. **151**: 468–479. doi:10.1111/ppl.12137

Fiorini, S., J. J. Middelburg, and J. P. Gattuso. 2011. Effects of elevated CO_2 partial pressure and temperature on the coccolithophore *Syracosphaera pulchra*. Aquat. Microb. Ecol. **64**: 221–232. doi:10.3354/ame01520

Fukuda, S. Y., Y. Suzuki, and Y. Shiraiwa. 2014. Difference in physiological responses of growth, photosynthesis and calcification of the coccolithophore *Emiliania huxleyi* to acidification by acid and CO_2 enrichment. Photosynth. Res. **121**: 299–309. doi:10.1007/s11120-014-9976-9

Gao, K., and others. 2012. Rising CO_2 and increased light exposure synergistically reduce marine primary productivity. Nat. Clim. Chang. **2**: 519–523. doi:10.1038/nclimate1507

Giordano, M., J. Beardall, and J. A. Raven. 2005. CO_2 concentrating mechanisms in Algae: Mechanisms, environmental modulation, and evolution. Ann. Rev. Plant Biol. **56**: 99–131. doi:10.1146/annurev.arplant.56.032604.144052

Guillard, R. R. L., and J. H. Ryther. 1962. Studies of marine planktonic diatoms. Can. J. Microbiol. **8**: 229–239. doi:10.1139/m62-029

Holligan, P. M., and others. 1993. A biogeochemical study of the coccolithophore, *Emiliania huxleyi*, in the North-Atlantic. Global Biogeochem. Cycles **7**: 879–900. doi:10.1029/93GB01731

Holtz, L. M., D. A. Wolf-Gladrow, and S. Thoms. 2015a. Simulating the effects of light intensity and carbonate system composition on particulate organic and inorganic carbon production in *Emiliania huxleyi*. J. Theor. Biol. **372**: 192–204. doi:10.1016/j.jtbi.2015.02.024

Holtz, L. M., D. A. Wolf-Gladrow, and S. Thoms. 2015b. Numerical cell model investigating cellular carbon fluxes in *Emiliania huxleyi*. J. Theor. Biol. **364**: 305–315. doi:10.1016/j.jtbi.2014.08.040

Hönisch, B., and others. 2012. The geological record of ocean acidification. Science **335**: 1058–1063.

Hoppe, C. J. M., L.-M. Holtz, S. Trimborn, and B. Rost. 2015. Ocean acidification decreases the light use efficiency in an Antarctic diatom under dynamic but not constant light. New Phytol. **207**: 159–171. doi:10.1111/nph.13334

Iglesias-Rodriguez, M. D., and others. 2008. Phytoplankton calcification in a high-CO_2 world. Science **320**: 336–340. doi:10.1126/science.1154122

Jin, P., K. Gao, and J. Beardall. 2013a. Evolutionary responses of a coccolithophorid *Gephyrocapsa oceanica* to ocean acidification. Evolution **67**: 1869–1878. doi:10.1111/evo.12112

Jin, P., K. Gao, V. E. Villafane, D. A. Campbell, and E. W. Helbling. 2013b. Ocean acidification alters the photosynthetic responses of a coccolithophorid to fluctuating ultraviolet and visible radiation. Plant Physiol. **162**: 2084–2094. doi:10.1104/pp.113.219543

Knap, A., A. Michaels, A. Close, H. Ducklow, and A. Dickson. 1996. Protocols for the joint global ocean flux study (JGOFS) core measurements, p. 1–170. Reprint of the IOC Manuals and Guides No. 29. UNESCO 1994.

Kottmeier, D. M., S. D. Rokitta, P. D. Tortell, and B. Rost. 2014. Strong shift from HCO_3^- to CO_2 uptake in *Emiliania huxleyi* with acidification: New approach unravels acclimation versus short-term pH effects. Photosynth. Res. **121**: 265–275. doi:10.1007/s11120-014-9984-9

Kottmeier, D. M., S. D. Rokitta, and B. Rost. 2016. Acidification, not carbonation, is the major regulator of carbon fluxes in the coccolithophore *Emiliania huxleyi*. New Phytol. **211**: 126–137. doi:10.1111/nph.13885

Kroeker, K. J., and others. 2013. Impacts of ocean acidification on marine organisms: Quantifying sensitivities and interaction with warming. Glob. Chang. Biol. **19**: 1884–1896. doi:10.1111/gcb.12179

Langer, G., M. Geisen, K. H. Baumann, J. Kläs, U. Riebesell, S. Thoms, and J. R. Young. 2006. Species-specific responses of calcifying algae to changing seawater carbonate chemistry. Geochem. Geophys. Geosyst. **7**: 1–12. doi:10.1029/2005GC001227.

Langer, G., G. Nehrke, I. Probert, J. Ly, and P. Ziveri. 2009. Strain-specific responses of *Emiliania huxleyi* to changing seawater carbonate chemistry. Biogeosciences **6**: 2637–2646. doi:10.5194/bg-6-2637-2009

Lefebvre, S. C., and others. 2012. Nitrogen source and pCO_2 synergistically affect carbon allocation, growth and morphology of the coccolithophore *Emiliania huxleyi*: Potential implications of ocean acidification for the carbon cycle. Glob. Chang. Biol. **18**: 493–503. doi:10.1111/j.1365-2486.2011.02575.x

Lohbeck, K. T., U. Riebesell, and T. B. Reusch. 2012. Adaptive evolution of a key phytoplankton species to ocean acidification. Nat. Geosci. **5**: 346–351. doi:10.1038/ngeo1441

Mackinder, L., G. Wheeler, D. Schroeder, U. Riebesell, and C. Brownlee. 2010. Molecular mechanisms underlying calcification in coccolithophores. Geomicrobiol. J. **27**: 585–595. doi:10.1080/01490451003703014

Mehrbach, C., C. H. Culberson, J. E. Hawley, and R. M. Pytkowicz. 1973. Measurement of the apparent dissociation constants of carbonic acid in seawater at atmospheric pressure. Limnol Oceanogr **18**: 897–907. doi:10.4319/lo.1973.18.6.0897

Meyer, J., and U. Riebesell. 2015. Reviews and syntheses: Responses of coccolithophores to ocean acidification: A meta-analysis. Biogeosciences **12**: 1671–1682. doi:10.5194/bg-12-1671-2015

Müller, M. N., T. W. Trull, and G. M. Hallegraeff. 2015. Differing responses of three Southern Ocean *Emiliania huxleyi* ecotypes to changing seawater carbonate chemistry. Mar. Ecol. Prog. Ser. **531**: 81–90. doi:10.3354/meps11309

Nanninga, H. J., and T. Tyrrell. 1996. Importance of light for the formation of algal blooms by *Emiliania huxleyi*. Mar. Ecol. Prog. Ser. **136**: 195–203. doi:10.3354/meps136195

Nielsen, M. V. 1997. Growth, dark respiration and photosynthetic parameters of the coccolithophorid *Emiliania huxleyi* (Prymnesiophyceae) acclimated to different day length-irradiance combinations. J. Phycol. **33**: 818–822. doi:10.1111/j.0022-3646.1997.00818.x

Paasche, E. 1964. A tracer study of the inorganic carbon uptake during coccolith formation and photosynthesis in the coccolithophorid *Coccolithus huxleyi*. Scandinavian Society for Plant Physiology.

Paasche, E. 1998. Roles of nitrogen and phosphorus in coccolith formation in *Emiliania huxleyi* (Prymnesiophyceae). Eur. J. Phycol. **33**: 33–42. doi:10.1017/S0967026297001480

Paasche, E., and S. Brubak. 1994. Enhanced calcification in the coccolithophorid *Emiliania huxleyi* (Haptophyceae) under phosphorus limitation. Phycologia **33**: 324–330. doi:10.2216/i0031-8884-33-5-324.1

Pierrot, D., E. Lewis, and D. Wallace. 2006. MS Excel program developed for CO_2 system calculations. ORNL/CDIAC-105. Carbon Dioxide Information Analysis Center, Oak Ridge National Laboratory, US Department of Energy, Oak Ridge, Tennessee.

Price, G. D., M. R. Badger, F. J. Woodger, and B. M. Long. 2008. Advances in understanding the cyanobacterial CO_2-concentrating-mechanism (CCM): Functional components, C_i transporters, diversity, genetic regulation and prospects for engineering into plants. J. Exp. Bot. **59**: 1441–1461. doi:10.1093/jxb/erm112

Ragni, M., R. L. Airs, N. Leonardos, and R. J. Geider. 2008. Photoinhibition of PSII in *Emiliania huxleyi* (Haptophyta) under high light stress: The roles of photoacclimation, photoprotection, and photorepair. J. Phycol. **44**: 670–683. doi:10.1111/j.1529-8817.2008.00524.x

Raitsos, D., S. Lavender, Y. Pradhan, T. Tyrrell, P. Reid, and M. Edwards. 2006. Coccolithophore bloom size variation in response to the regional environment of the subarctic North Atlantic. Limnol. Oceanogr. **51**: 2122–2130. doi:10.4319/lo.2006.51.5.2122

Raven, J., and K. Crawfurd. 2012. Environmental controls on coccolithophore calcification. Mar. Ecol. Prog. Ser. **470**: 137–166. doi:10.3354/meps09993

Raven, J. A., and J. Beardall. 2016. The ins and outs of CO_2. J. Exp. Bot. **67**: 1–13. doi:10.1093/jxb/erv451

Read, B. A., and others. 2013. Pan genome of the phytoplankton *Emiliania* underpins its global distribution. Nature **499**: 209–213. doi:10.1038/nature12221

Rickaby, R. E., and others. 2016. Environmental carbonate chemistry selects for phenotype of recently isolated strains of *Emiliania huxleyi*. Deep-Sea Res. Part II Top. Stud. Oceanogr. **127**: 28–40. doi:10.1016/j.dsr2.2016.02.010

Riebesell, U., I. Zondervan, B. Rost, P. D. Tortell, E. Zeebe, and F. M. M. Morel. 2000. Reduced calcification in marine plankton in response to increased atmospheric CO_2. Nature **407**: 634–637. doi:10.1038/35030078

Rokitta, S., and B. Rost. 2012. Effects of CO_2 and their modulation by light in the life-cycle stages of the coccolithophore *Emiliania huxleyi*. Limnol. Oceanogr. **57**: 607–618. doi:10.4319/lo.2012.57.2.0607

Rokitta, S., U. John, and B. Rost. 2012. Ocean acidification affects redox-balance and ion-homeostasis in the life-cycle stages of *Emiliania huxleyi*. PLOS ONE **7**: e52212. doi:10.1371/journal.pone.0052212

Rost, B., I. Zondervan, and U. Riebesell. 2002. Light-dependent carbon isotope fractionation in the coccolithophorid *Emiliania huxleyi*. Limnol. Oceanogr. **47**: 120–128. doi:10.4319/lo.2002.47.1.0120

Rost, B., and U. Riebesell. 2004. Coccolithophores and the biological pump: Responses to environmental changes, p. 76–99. In H. R. Thierstein and J. R. Young [eds.], Coccolithophores—from molecular processes to global impact. Springer.

Rost, B., U. Riebesell, and D. Sültemeyer. 2006. Carbon acquisition of marine phytoplankton: Effect of photoperiod length. Limnol. Oceanogr. **51**: 12–20. doi:10.4319/lo.2006.51.1.0012

Schulz, K. G., B. Rost, S. Burkhardt, U. Riebesell, S. Thoms, and D. A. Wolf-Gladrow. 2007. The effect of iron availability on the regulation of inorganic carbon acquisition in the coccolithophore *Emiliania huxleyi* and the significance of cellular compartmentation for stable carbon isotope fractionation. Geochim. Cosmochim. Acta **71**: 5301–5312. doi:10.1016/j.gca.2007.09.012

Sett, S., L. T. Bach, K. G. Schulz, S. Koch-Klavsen, M. Lebrato, and U. Riebesell. 2014. Temperature modulates coccolithophorid sensitivity of growth, photosynthesis and calcification to increasing seawater pCO_2. PLOS ONE **9**: e88308. doi:10.1371/journal.pone.0088308

Sikes, C. S., R. D. Roer, and K. M. Wilbur. 1980. Photosynthesis and coccolith formation: Inorganic carbon sources

and net inorganic reaction of deposition. Limnol. Oceanogr. **25**: 248–261. doi:10.4319/lo.1980.25.2.0248

Stanley, S. M., J. B. Ries, and L. A. Hardie. 2005. Seawater chemistry, coccolithophore population growth, and the origin of Cretaceous chalk. Geology **33**: 593. doi:10.1130/G21405.1

Stoll, M. H. C., K. Bakker, G. H. Nobbe, and R. R. Haese. 2001. Continuous-flow analysis of dissolved inorganic carbon content in seawater. Anal. Chem. **73**: 4111–4116. doi:10.1021/ac010303r

Suffrian, K., K. G. Schulz, M. A. Gutowska, U. Riebesell, and M. Bleich. 2011. Cellular pH measurements in *Emiliania huxleyi* reveal pronounced membrane proton permeability. New Phytol. **190**: 595–608. doi:10.1111/j.1469-8137.2010.03633.x

Taylor, A. R., A. Chrachri, G. Wheeler, H. Goddard, and C. Brownlee. 2011. A voltage-gated H^+ channel underlying pH homeostasis in calcifying coccolithophores. PLOS Biol **9**: e1001085. doi:10.1371/journal.pbio.1001085

Tchernov, D., M. Hassidim, B. Luz, A. Sukenik, L. Reinhold, and A. Kaplan. 1997. Sustained net CO_2 evolution during photosynthesis by marine microorganisms. Curr. Biol. **7**: 723–728. doi:10.1016/S0960-9822(06)00330-7

Trimborn, S., G. Langer, and B. Rost. 2007. Effect of varying calcium concentrations and light intensities on calcification and photosynthesis in *Emiliania huxleyi*. Limnol. Oceanogr. **52**: 2285–2293. doi:10.4319/lo.2007.52.5.2285

Tyrrell, T., and A. Merico. 2004. *Emiliania huxleyi*: Bloom observations and the conditions that induce them, In H. R. Thierstein and J. R. Young [eds.], Coccolithophores—from molecular processes to global impact. Springer.

Van Bleijswijk, J. D., R. S. Kempers, M. J. Veldhuis, and P. Westbroek. 1994. Cell and growth characteristics of types A and B of *Emiliania huxleyi* (Prymnesiophyceae) as determined by flow cytometry and chemical analyses. J. Phycol. **30**: 230–241. doi:10.1111/j.0022-3646.1994.00230.x

Wolf-Gladrow, D. A., U. Riebesell, S. Burkhardt, and J. Bijma. 1999. Direct effects of CO_2 concentration on growth and isotopic composition of marine plankton. Tellus B **51**: 461–476. doi:10.1034/j.1600-0889.1999.00023.x

Xing, T., K. Gao, and J. Beardall. 2015. Response of growth and photosynthesis of *Emiliania huxleyi* to visible and UV irradiances under different light regimes. Photochem. Photobiol. **91**: 343–349. doi:10.1111/php.12403

Xu, K., and K. Gao. 2015. Solar UV Irradiances modulate effects of ocean acidification on the coccolithophorid *Emiliania huxleyi*. Photochem. Photobiol. **91**: 92–101. doi:10.1111/php.12363

Zeebe, R. E., and D. A. Wolf-Gladrow. 2001. CO_2 in seawater: Equilibrium, kinetics, isotopes. Elsevier Science B.V.

Zhang, Y., L. T. Bach, K. G. Schulz, and U. Riebesell. 2015. The modulating effect of light intensity on the response of the coccolithophore *Gephyrocapsa oceanica* to ocean acidification. Limnol. Oceanogr. **60**: 2145–2157. doi:10.1002/lno.10161

Zondervan, I. 2007. The effects of light, macronutrients, trace metals and CO_2 on the production of calcium carbonate and organic carbon in coccolithophores—a review. Deep-Sea Res. Pt II **54**: 521–537. doi:10.1016/j.dsr2.2006.12.004

Zondervan, I., B. Rost, and U. Riebesell. 2002. Effect of CO_2 concentration on the PIC/POC ratio in the coccolithophore *Emiliania huxleyi* grown under light-limiting conditions and different daylengths. J. Exp. Mar. Biol. Ecol. **272**: 55–70. doi:10.1016/S0022-0981(02)00037-0

Acknowledgments

We thank Christian Großmann for supporting us with the culture work, carbonate chemistry measurements and cell harvesting, and Klaus-Uwe Richter and David Stronzek for the technical support with the mass spectrometer. Our thanks also go to Beate Müller, Ulrike Richter and Anja Terbrüggen for measuring the DIC, ANCA and nutrient samples. The interpretation of our data strongly profited from the fruitful discussions with Lena Holtz. We also acknowledge the feedback of the two anonymous reviewers. The project was financially supported by funding from the German Federal Ministry for Education and Research (BMBF) in the framework of the project Bioacid II (03F0655B) and ZeBiCa^2 (031A518C).

Submitted 24 March 2016
Revised 12 May 2016
Accepted 16 May 2016

Associate editor: James Falter